Bloch-like energy oscillations

Axel Gagge and Jonas Larson
Department of Physics, Stockholm University, AlbaNova University Center, 106 91 Stockholm, Sweden

(Received 1 September 2018; published 13 November 2018)

We identify a type of periodic evolution that appears in driven quantum systems. Provided that the instantaneous (adiabatic) energies are equidistant we show how such systems can be mapped to (time-dependent) tilted single-band lattice models. Having established this mapping, the dynamics can be understood in terms of Bloch oscillations in the instantaneous energy basis. In our lattice model the site-localized states are the adiabatic ones, and the Bloch oscillations manifest as a periodic repopulation among these states, or equivalently a periodic change in the system's instantaneous energy. Our predictions are confirmed by considering two different models: a driven harmonic oscillator and a Landau-Zener grid model. To strengthen the link between our energy Bloch oscillations and the original spatial Bloch oscillations we add a random disorder that breaks the translational invariance of the spectrum. This verifies that the oscillating evolution breaks down and instead turns into a diffusive spreading. Finally, we consider a trapped ion setup and demonstrate how the mechanism can be utilized to prepare motional cat state of the ion.

DOI: 10.1103/PhysRevA.98.053820

I. INTRODUCTION

Periodic driving of closed quantum systems typically leads to heating [1] and, in some cases, that the steady state approaches infinite temperature. The time-dependent drive induces a coupling between nearby energy eigenstates, and consequently the system shows an energy diffusion. Such behavior is especially expected in quantum many-body systems, or for systems showing large anharmonicities in its spectrum. However, for some integrable systems a periodical driving may not lead to an infinite temperature steady state, but a periodical solution. A prime example is the driven harmonic oscillator when employing the rotating wave approximation [2].

The harmonic oscillator is also the text-book example of a closed (undriven) quantum system showing periodic evolution. After multiples of the classical period $2\pi/\omega$ (with ω the oscillator frequency) we regain perfect revivals of the initial state. This is the result of the equidistant energy spectrum; all probability amplitudes return back in phase at these instances. A less-known example of a closed system with an equidistant spectrum is that of a tilted single-band lattice model. The spectrum forms a so-called Wannier-Stark ladder, unbounded from below and above [3]. A particle in such a tilted lattice will not continuously accelerate (as it would classically), but rather show a periodic motion called Bloch oscillation. By now, Bloch oscillations have been demonstrated in numerous systems [4]. In real experimental systems, however, the single-band assumption is not strictly true, and the Bloch oscillations will eventually die out.

In this work we discuss a type of periodic evolution that we term "energy Bloch oscillations." Instead of displaying a real-space oscillating behavior, in our case the system's energy will be oscillating. Thus, we consider a time-dependent system where energy is not conserved. If the spectrum of the undriven system is equidistant, then by expressing the full Hamiltonian in the adiabatic basis we find a "tilted" single-band model. The site localized states of the original Bloch Hamiltonian have been replaced by energy localized adiabatic states, and thereby the manifestation of oscillations in the system's energy. The difference compared to the original lattice Bloch model is that we have time-dependent parameters. As we show, despite this we still find perfect periodic evolution. However, the oscillations may, in some cases, be more reminiscent of "super Bloch oscillations" that appear in driven tilted lattices [5,6]. To verify our predictions we consider two different models, the driven harmonic oscillator [7] and a Landau-Zener grid [8–10]. In both examples we find clear evidence of energy Bloch oscillations. We also show how the oscillations break down when we relax the assumption of an equidistant spectrum. This leads to diffusive spreading among the adiabatic energy states. As an application of our results we imagine a trapped ion system and demonstrate how motional cat states can be prepared.

The outline of the paper is as follows. Section II is devoted to the general theory, starting with recapitulating the basics of Bloch oscillations and super Bloch oscillations in the single-band model, and then presenting the formal description of energy Bloch oscillations. Section III discusses the two examples, the driven harmonic oscillator in Sec. III A and the Landau-Zener grid model in Sec. III B. In Sec. IV it is shown how the method is used to prepare nonclassical states. Finally, we summarize in Sec. V and give a discussion about experimental relevance.

II. GENERAL THEORY

A. Prelude—Bloch oscillations

Traditionally there are two different approaches for understanding the dynamics of a particle in a periodic potential and exposed to a constant force. The *acceleration theorem*

says that in the adiabatic regime the quasimomentum k grows linearly in time; $k(t) = k_0 + Ft$. We may thereby think in terms of the untilted model with a time-dependent quasimomentum. For a single band, the energy is given by a band $\varepsilon(k)$ defined within the first Brillouin zone, and the dynamics is then explained via the substitution $\varepsilon(k) \to \varepsilon(k_0 + Ft)$. If the initial state is localized in momentum, the wave-packet evolves with a group velocity $v_g(t) = \partial\varepsilon(k)/\partial k|_{k=k_0+Ft}$. Since quasimomentum is defined over the periodic Brillouin zone, the oscillating evolution follows [11]. The other approach is by introducing so-called Wannier-Stark ladders (one ladder for each band), which are complex equidistant energies [3]. The decay of the Bloch oscillations stems from Zener tunneling between different energy bands—in the language of the acceleration theorem it marks the breakdown of adiabaticity, while in the Wannier-Stark approach the decay is reflected in the size of the imaginary parts of the spectrum. Then, for a single-band model there are no additional bands generating Zener tunnelings, and the oscillations will sustain indefinitely. For a tight-binding model we let J denote the tunneling amplitude between adjacent sites, and ω the onsite energy shift representing the applied force, i.e. ($\hbar = 1$ throughout),

$$\hat{H}_{\mathrm{sb}} = -J \sum_{n=-\infty}^{+\infty} (|n\rangle\langle n+1| + |n+1\rangle\langle n|) + \omega \sum_{n=-\infty}^{+\infty} n|n\rangle\langle n|. \tag{1}$$

Here $|n\rangle$ represents the Wannier state localized at site n. The energies are [12]

$$E_m = m\omega, \quad m \in \mathbb{Z}, \tag{2}$$

which form the Wannier-Stark ladder (the vanishing imaginary part implies that the oscillations do not decay, as expected in this single band model). Note that the energies are independent of J in the limit of an infinite lattice as considered here. The eigenstates depend, however, on J [13]

$$|\psi_m\rangle = \sum_{n=-\infty}^{+\infty} J_{n-m}(2J/\omega)|n\rangle, \tag{3}$$

where $J_{n-m}(2J/\omega)$ is the Bessel function of the first kind. $J_{n-m}(2J/\omega)$ quickly vanishes for $|n-m| \gg 2J/\omega$. Hence, the eigenstates are localized in contrast to the extended Bloch states (the localization length diverges as $1/\omega$ though).

With the equidistant spectrum Eq. (2) it is clear that after a period $T_{\mathrm{Bloch}} = 2\pi/\omega$, all energy eigenstates have regained their original phase and there is a perfect revival of the initial state. We may typically envision two types of initial states: those localized in real space or those localized in momentum space. In the latter case we regain the typical oscillating behavior of the wave-packet in real space, while in the other case we get the so called breathing modes. Examples of both the breathing and the oscillating modes for the single-band tight-binding model Eq. (1) are presented in Fig. 1. Shown is the density

$$P_n(t) = |\langle n|\psi(t)\rangle|^2, \tag{4}$$

with the initial condition $|\psi(0)\rangle = |0\rangle$ for Fig. 1(a) and a Gaussian centered around $n = 0$ with width $\sigma = 10$ for Fig. 1(b).

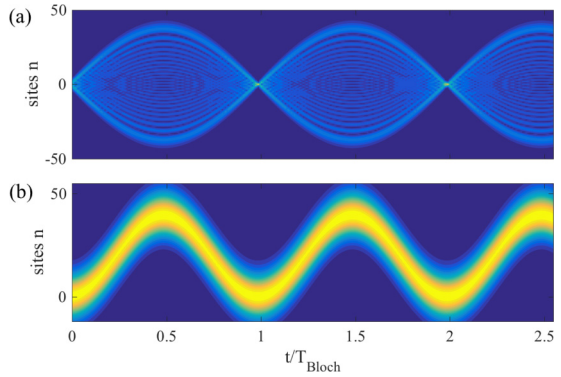

FIG. 1. Time-evolution of the probability density $\sqrt{P_n(t)}$ for the model Eq. (1). Shown is the breathing mode (a) and the oscillating mode (b). The reason for plotting the square-root of $P_n(t)$ is to better visualize the weakly populated sites. For the breathing mode the initial state populates only the site $n = 0$, while for the oscillating mode the initial state is a Gaussian with a width $\sigma = 10$ (i.e., it populates ∼40 sites). The revivals at multiples of the Bloch period $T_{\mathrm{Bloch}} = 2\pi/\omega$ is evident. The width of the wave packet for the breathing mode and the amplitude for the oscillating mode is determined by $\frac{4J}{\omega}|\sin(t/T_{\mathrm{Bloch}})|$ [12]. The dimensionless parameters used for this figure are $J = 10$ and $\omega = 1$.

Phenomena arise when the lattice, apart from being tilted, is periodically driven. For an untilted lattice the tunneling J is renormalized by a Bessel function [14]. The argument of the Bessel function depends on the parameters of the drive, and if these are tuned such that the Bessel function is zero, the tunneling is fully suppressed leading to a so called Bloch band collapse [15]. Thus, the particle transport may be greatly influenced by the drive. When the lattice is tilted, there occur resonances between the drive frequency Ω and corresponding frequencies between the Wannier-Stark energies Eq. (2), i.e.,

$$\delta\Omega_n = \Omega - n\omega, \quad n = 1,\ 2,\ 3, \ldots. \tag{5}$$

This is similar to the red/blue sideband driving in trapped ion physics [16]. For the tilted lattice a beating between the involved frequencies takes place which may result in extended motion in the lattice [5,6]. In particular, super Bloch oscillations describe oscillating motion that may cover hundreds of lattice sites provided that $\delta\Omega_n$ is small for some integer n. The period for the super Bloch oscillation then becomes $T_{\mathrm{sBloch}} = 2\pi/\delta\Omega_n$ and the amplitude scales as $\sim J/\delta\Omega_n$ (instead of $\sim J/\omega$ for regular Bloch oscillations).

B. Periodically driven quantum systems

We consider some driven system

$$\hat{H}(t) = \hat{H}_0 + \hat{V}(t), \tag{6}$$

where the drive is periodic with a period T, $\hat{V}(t) = \hat{V}(t+T)$, and the two terms of the Hamiltonian in general do not commute, i.e., $[\hat{H}_0, \hat{V}(t)] \neq 0$. Furthermore, the spectrum of the bare Hamiltonian $\hat{H}_0$ has the equidistant form $E_n = n\omega$ with $n \in \mathbb{Z}$ (we take n to run over both positive and negative integers, but we could impose a lower bound $n = 0$ as in the example of the driven oscillator in the next section). The

adiabatic states are the instantaneous eigenstates of $\hat{H}(t)$,

$$\hat{H}(t)\left|\psi_n^{(\mathrm{ad})}(t)\right\rangle = E_n^{(\mathrm{ad})}(t)\left|\psi_n^{(\mathrm{ad})}(t)\right\rangle, \tag{7}$$

and $E_n^{(\mathrm{ad})}(t)$ are the adiabatic energies. With the state $|\psi_n^{(\mathrm{ad})}(t)\rangle$ we may form a time-dependent unitary $\hat{U}(t)$ that diagonalizes $\hat{H}(t)$. This defines a change of basis $|\tilde{\psi}(t)\rangle = \hat{U}(t)|\psi(t)\rangle$, but since $\hat{U}(t)$ is time-dependent it will induce a 'gauge term' $\hat{A}(t)$ in the transformed Schrödinger equation,

$$i\,\partial_t|\tilde{\psi}(t)\rangle = [\hat{D}(t) - \hat{A}(t)]|\tilde{\psi}(t)\rangle. \tag{8}$$

Here the diagonal

$$\hat{D}(t) = \mathrm{diag}\big[E_m^{(\mathrm{ad})}(t)\big], \tag{9}$$

and the gauge potential

$$\hat{A}(t) = i\hat{U}(t)\partial_t\hat{U}^\dagger(t). \tag{10}$$

This last term is also called the nonadiabatic coupling term or the Berry connection [17,18] depending on the community. Its matrix elements expressed in the adiabatic basis are

$$[\hat{A}(t)]_{mn} = i\left\langle\psi_m^{(\mathrm{ad})}(t)\right|\partial_t\left|\psi_n^{(\mathrm{ad})}(t)\right\rangle \equiv \Theta_{mn}(t). \tag{11}$$

We can choose a gauge (the adiabatic states are defined up to an overall time-dependent phase factor [17,18]) such that $\Theta_{nn}(t) = 0$. It should be clear that $\hat{A}(t)$ is responsible for the coupling of different adiabatic states, and that the adiabatic approximation consists in setting $\hat{A}(t) = 0$.

The driving $\hat{V}(t)$ is chosen such that the adiabatic energies fulfill (up to a possible overall constant shift)

$$\epsilon_n \equiv \frac{1}{T}\int_0^T E_n^{(\mathrm{ad})}(t)dt = n\omega. \tag{12}$$

Hence, the driving constitutes a "dressing" of the bare energies E_m that averages to zero over one period. Given this property we see that (for $n \neq m$)

$$\begin{aligned}\Theta_{mn}(t) &= i\left\langle\psi_m^{(\mathrm{ad})}(t)\right|\partial_t\left|\psi_n^{(\mathrm{ad})}(t)\right\rangle \\ &= \frac{\left\langle\psi_m^{(\mathrm{ad})}(t)\right|(\partial_t\hat{V}(t))\left|\psi_n^{(\mathrm{ad})}(t)\right\rangle}{E_m^{(\mathrm{ad})}(t) - E_n^{(\mathrm{ad})}(t)} \sim \frac{1}{m-n},\end{aligned} \tag{13}$$

i.e., the nonadiabatic coupling typically falls off as $(m-n)^{-1}$. In general, we also have $\Theta_{mn}(t) = \Theta_{m-n}(t)$. In other words, the element $\Theta_1(t)$ will dominate the nonadiabatic term $\hat{A}(t)$. Using the above, the Hamiltonian can be written as

$$\begin{aligned}\hat{H}(t) = &\sum_{l=1}^{\infty}\sum_{n=-\infty}^{+\infty}\Theta_l(t)\left(\left|\psi_n^{(\mathrm{ad})}(t)\right\rangle\left\langle\psi_{n+l}^{(\mathrm{ad})}(t)\right| + \mathrm{H.c.}\right) \\ &+ \sum_{n=-\infty}^{+\infty}E_n^{(\mathrm{ad})}(t)\left|\psi_n^{(\mathrm{ad})}(t)\right\rangle\left\langle\psi_n^{(\mathrm{ad})}(t)\right|,\end{aligned} \tag{14}$$

where H.c. stands for Hermitian conjugate. When restricting the nonadiabatic couplings to $\Theta_1(t)$ the adiabatic Hamiltonian becomes

$$\begin{aligned}\hat{H}(t) \approx &\,\Theta_1(t)\sum_{n=-\infty}^{+\infty}\left(\left|\psi_n^{(\mathrm{ad})}(t)\right\rangle\left\langle\psi_{n+1}^{(\mathrm{ad})}(t)\right| + \mathrm{H.c.}\right) \\ &+ \sum_{n=-\infty}^{+\infty}E_n^{(\mathrm{ad})}(t)\left|\psi_n^{(\mathrm{ad})}(t)\right\rangle\left\langle\psi_n^{(\mathrm{ad})}(t)\right|.\end{aligned} \tag{15}$$

By comparing this expression to the Hamiltonian Eq. (1) a mapping between the two models is evident via the following correspondence:

$$|n\rangle \leftrightarrow \left|\psi_n^{(\mathrm{ad})}(t)\right\rangle, \quad J \leftrightarrow \Theta_1(t), \quad n\omega \leftrightarrow E_n^{(\mathrm{ad})}(t). \tag{16}$$

And similarly, Eq. (4) takes the form

$$P_n(t) = \left|\left\langle\psi_n^{(\mathrm{ad})}(t)\right|\psi(t)\right\rangle\right|^2. \tag{17}$$

What we have found is that in the periodically driven model the site localized Wannier states $|n\rangle$ have been replaced by the adiabatic states $|\psi_n^{(\mathrm{ad})}(t)\rangle$, which instead are perfectly localized in energy. Without the time-dependence the mapping is exact.

Note that the fact that we neglected couplings beyond "nearest neighbors" does not change our argument, indeed the Bloch oscillations still persist with higher-order terms as these would only affect the actual shape and amplitudes of the oscillations. The time-averaged energy gap $\delta_n = \epsilon_{n+1} - \epsilon_n$ $(= \omega)$ is clearly translational invariant in the subscript n. This property suggests, just as for the Wannier-Stark ladder, that we should find a revival in the system state after a time $T_{\mathrm{EBloch}} = 2\pi/\omega$ (where the subscript EBloch denotes that the period occurs in the energy space and not in the real space). The resulting periodic evolution defines the energy Bloch oscillations. Since the Hamiltonian is periodic with period T, we must have $E_n^{(\mathrm{ad})}(t) = E_n^{(\mathrm{ad})}(t+T)$ and $\Theta_l(t) = \Theta_l(t+T)$. Hence, if $T_{\mathrm{EBloch}} \gg T$ we may expect that the evolution implies an inherent averaging of the parameters such that the Bloch oscillations should be almost perfect as in Fig. 1. However, the time-dependence of the parameters could in principle give rise to some sort of super Bloch oscillations due to beating of different characteristic frequencies. In this respect, our model bears similarities with the driven Bloch oscillation problem discussed in the previous subsection.

Let us give a final comment on the link between the two models defined by the Hamiltonian Eqs. (1) and (15). We pointed out in the previous subsection that Bloch oscillations may be understood from the acceleration theorem, which states that the quasimomentum k grows linearly in time, and since the quasimomentum can be restricted to the first Brillouin zone a periodic motion results (every time the quasimomentum hits the end of the Brillouin zone it reenters on the opposite side). Now what would be the counterpart of this behavior in our model? The answer is that the Floquet quasienergy ε_n, bounded to $(\omega/2, \omega/2]$ (corresponding Brillouin zone), replaces the quasimomentum [19].

III. EXAMPLES

A. Driven harmonic oscillator

The first system that comes to mind having an equidistant spectrum is the harmonic oscillator. The Hamiltonian for the periodically driven oscillator is taken as

$$\hat{H}_{\mathrm{dHO}}(t) = \omega\hat{a}^\dagger\hat{a} + J\frac{\hat{a}^\dagger + \hat{a}}{\sqrt{2}}\sin(\Omega t), \tag{18}$$

where the creation and annihilation operators obey the regular Bosonic commutation $[\hat{a}, \hat{a}^\dagger] = 1$, and act on the n-Boson Fock states as $\hat{a}^\dagger|n\rangle = \sqrt{n+1}|n+1\rangle$ and $\hat{a}|n\rangle = \sqrt{n}|n-1\rangle$.

The first part corresponds to $\hat{H}_0$ and the second term to $\hat{V}(t)$ of Eq. (6). Alternatively, we may consider the quadrature representation defined by $\hat{x} = \frac{\hat{a}+\hat{a}^\dagger}{\sqrt{2}}$ and $\hat{p} = -i\frac{\hat{a}-\hat{a}^\dagger}{\sqrt{2}}$, for which the Hamiltonian takes the form

$$\hat{H}_{\mathrm{dHO}}(t) = \omega\frac{\hat{p}^2+\hat{x}^2}{2} + J\hat{x}\sin(\Omega t), \tag{19}$$

Even though the full time-dependent problem is analytically solvable [7], here we are more interested in expressing the Hamiltonian in the adiabatic basis. Nevertheless, one important general observation is that since the Hamiltonian is quadratic in the Boson operators any initial Gaussian state will stay Gaussian when evolved with this Hamiltonian. In particular, a coherent state remains coherent for all times. This is certainly also true when one would apply the rotating wave approximation to the above model [20]. However, contrary to that situation, without the rotating wave approximation the amplitude of the coherent state will not stay constant—a necessity to observe the energy Bloch oscillations.

By noticing that the $\hat{H}_{\mathrm{dHO}}(t)$ is nothing but a displaced oscillator it is convenient to introduce the displacement operator,

$$\hat{D}[J\sin(\Omega t)/\omega] = \exp[-i\hat{p}J\sin(\Omega t)/\omega], \tag{20}$$

which transforms the Hamiltonian into

$$\begin{aligned}\hat{H}'_{\mathrm{dHO}}(t) &= \hat{D}[J\sin(\Omega t)/\omega]\hat{H}_{\mathrm{dHO}}(t)\hat{D}^\dagger[J\sin(\Omega t)/\omega]\\ &= \omega\frac{\hat{p}^2+[\hat{x}+J\sin(\Omega t)]^2}{2} - \frac{J^2}{2\omega}\sin^2(\Omega t).\end{aligned} \tag{21}$$

Thus, the adiabatic energies are just

$$E_n^{(\mathrm{ad})}(t) = \omega n - \frac{J^2\sin^2(\Omega t)}{2\omega}, \tag{22}$$

and the adiabatic states are $|\psi_n^{(\mathrm{ad})}(t)\rangle = \hat{D}(J\sin(\Omega t)/\omega)|n\rangle$ (i.e., displaced Fock states [21]). Using the second identity of Eq. (13) it is straightforward to also evaluate the nonadiabatic coupling terms

$$\begin{aligned}\Theta_{mn}(t) &= \frac{\langle\psi_m^{(\mathrm{ad})}(t)|[\partial_t\hat{V}(t)]|\psi_n^{(\mathrm{ad})}(t)\rangle}{E_m^{(\mathrm{ad})}(t)-E_n^{(\mathrm{ad})}(t)}\\ &= J\Omega\cos(\Omega t)\frac{\langle m|\hat{D}^\dagger[J\sin(\Omega t)/\omega]\hat{x}\hat{D}[J\sin(\Omega t)/\omega]|n\rangle}{(m-n)\omega}\\ &= J\Omega\cos(\Omega t)\frac{\langle m|[\hat{x}-J\sin(\Omega t)/\omega]|n\rangle}{(m-n)\omega}\\ &= \frac{J\Omega\cos(\Omega t)}{(m-n)\omega}\frac{\sqrt{n}\delta_{m,n-1}+\sqrt{n+1}\delta_{m,n+1}}{\sqrt{2}},\end{aligned} \tag{23}$$

where we have used that $m \neq n$. We note that in this special case only $\Theta_1(t)$ is nonzero, i.e., all couplings beyond "nearest neighbors" vanish. Summing up, the Hamiltonian in the adiabatic basis becomes

$$\begin{aligned}\hat{H}_{\mathrm{dHO}}(t) = &\frac{J\Omega\cos(\Omega t)}{\omega}\sum_{n=0}^{\infty}\left(|\psi_n^{(\mathrm{ad})}(t)\rangle\langle\psi_{n+1}^{(\mathrm{ad})}(t)| + \mathrm{H.c.}\right)\\ &+\sum_{n=0}^{\infty}\omega n|\psi_n^{(\mathrm{ad})}(t)\rangle\langle\psi_n^{(\mathrm{ad})}(t)|\end{aligned} \tag{24}$$

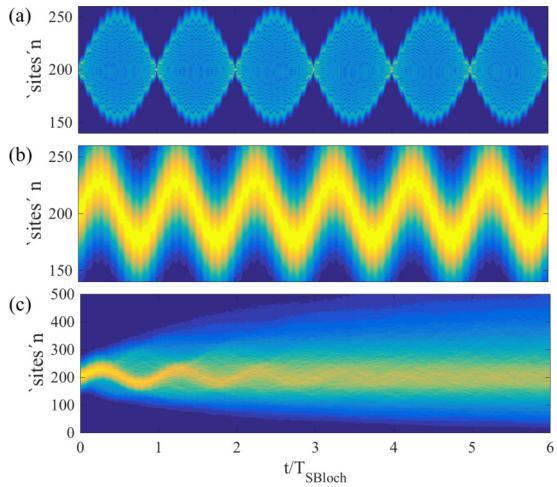

FIG. 2. The upper two plots, (a) and (b), display the probabilities $\sqrt{P_n(t)}$ for, respectively, an initial Fock state $|\psi(0)\rangle = |200\rangle$ and an initial coherent state $|\psi(0)\rangle = |\alpha\rangle$ with an amplitude $\alpha = \sqrt{200}$. The two cases correspond, respectively, to the breathing and oscillating modes. The appearance of Bloch oscillations is strikingly clear. In fact, for this model we regain perfect revivals. In the lower plot (c) we instead show the importance of the "translational invariance." A random shift ξ_n of the bare energies $E_n = \omega n$ have been included, with the random variable drawn from a Gaussian distribution centered around 0 and with a variance $\pi/50$. The initial state is the same as in (b), and we have averaged over 10 ξ_n-realizations. We can see traces of the Bloch oscillating motion at early times, but at later times the wave-packet spreads out indicating a heating. The dimensionless parameters are $\omega = 1$, $\Omega = 1.2$ (giving a Bloch period $T_{\mathrm{sEBloch}} = 2\pi/|\omega-\Omega| = 10\pi$), and $J = 0.5$.

up to an overall constant $-J^2\sin^2(\Omega t)/2$. Note that the sum does not run over negative n's since the harmonic oscillator is bounded from below. This "edge" of our lattice should not be a problem as long as we consider localized states with $\langle\hat{a}^\dagger\hat{a}\rangle \gg 1$.

At first sight, Eq. (24) seems to suggest that we should envision energy Bloch oscillations with a period $T_{\mathrm{EBloch}} = 2\pi/\omega$. However, the time-dependent tunneling amplitude results in that we instead find super Bloch oscillations with a period $T_{\mathrm{sEBloch}} = 2\pi/\delta\Omega = 2\pi/|\omega-\Omega|$. This is demonstrated in Figs. 2(a) and 2(b). These plots are the counterparts of those of Fig. 1, i.e., (a) shows the breathing mode and (b) the oscillating mode. For the oscillating mode we consider an initial coherent state $|\alpha\rangle$ (i.e., an eigenstate of the annihilation operator, $\hat{a}|\alpha\rangle = \alpha|\alpha\rangle$). The advantage with coherent states is that they are easy to prepare experimentally, in comparison to highly excited Fock states which was used for demonstrating the breathing mode.

Translational invariance is a necessity for Bloch oscillations to occur. In the original setting it gives rise to the quasimomentum restricted to the first Brillouin zone. For the energy Bloch oscillations, the translational invariance appears as the equidistant spectrum (and in a strict sense also in the $(m-n)$-dependence of the coupling terms $\Theta_{(m-n)}(t)$). If we break the translational invariance we expect also a breakdown of the energy Bloch oscillations. There are numerous ways

we can imagine to do this, for example by considering an anharmonic spectrum. Here we randomly shift the undriven harmonic oscillator energy levels

$$\hat{H}_0 = \sum_{n=0}^{\infty} (\omega n + \xi_n)|n\rangle\langle n|, \tag{25}$$

where ξ_n is a random variable drawn from a Gaussian distribution with zero mean and variance taken to be $\sigma = \pi/50$. The results are shown in Fig. 2(c), where we used the same initial coherent state and parameters as for plot (b) of the same figure. For short times we still see remnants of the Bloch oscillations. However, as time progresses the destructive interference between the different paths become evident and we see a spreading of the initially localized wave-packet such that more and more adiabatic states get populated. Numerically, we find a $\sqrt{t}$-broadening, which one can expect due to the loss of constructive interferences.

B. Landau-Zener grid

After the celebrated Landau-Zener model [22] there have been numerous generalizations of it to multilevel systems [8,9,23]. The one we consider forms a grid of Landau-Zener transitions in the energy-time plane, i.e., the adiabatic or diabatic energies forms a lattice as shown in Fig. 3(a). Such a structure is obtained from the Landau-Zener grid model defined by the Hamiltonian [8,9]

$$\hat{H}^{(\mathrm{d})}_{LZg}(t) = \omega(\hat{S}_z \otimes \mathbb{I}) + \lambda t(\mathbb{I} \otimes \hat{\sigma}_z) + J(\mathbb{A} \otimes \hat{\sigma}_x), \tag{26}$$

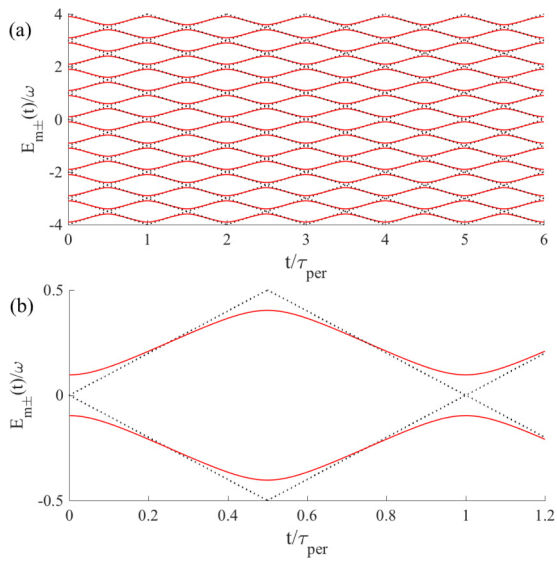

FIG. 3. Diabatic (dotted black lines) and adiabatic (solid red lies) energies. The upper plot (a) demonstrates the Landau-Zener grid in the energy-time plane, while the avoided crossings is more evident from the lower plot (b) that zooms in on two energies over one period τ_{per}.

where $\hat{\sigma}_x$ and $\hat{\sigma}_z$ are the regular Pauli matrices, $\hat{S}_z$ is a diagonal matrix with elements ..., -2, -1, 0, $+1$, $+2$, ..., and $\mathbb{A}$ is a matrix with all elements equal to one. The superscript d that labels the Hamiltonian is written in the diabatic basis (see below). Explicitly in the $\hat{\sigma}_z$ eigenbasis we have

$$\hat{H}^{(\mathrm{d})}_{LZg}(t) = \left[\begin{array}{ccccc|ccccc}
\ddots & \vdots & \vdots & \vdots & & \ddots & \vdots & \vdots & \vdots & \\
\cdots & +\omega+\lambda t & 0 & 0 & \cdots & \cdots & J & J & J & \cdots \\
\cdots & 0 & +\lambda t & 0 & \cdots & \cdots & J & J & J & \cdots \\
\cdots & 0 & 0 & -\omega+\lambda t & \cdots & \cdots & J & J & J & \cdots \\
 & \vdots & \vdots & \vdots & \ddots & & \vdots & \vdots & \vdots & \ddots \\
\hline
\ddots & \vdots & \vdots & \vdots & & \ddots & \vdots & \vdots & \vdots & \\
\cdots & J & J & J & \cdots & \cdots & +\omega-\lambda t & 0 & 0 & \cdots \\
\cdots & J & J & J & \cdots & \cdots & 0 & -\lambda t & 0 & \cdots \\
\cdots & J & J & J & \cdots & \cdots & 0 & 0 & -\omega-\lambda t & \cdots \\
 & \vdots & \vdots & \vdots & \ddots & & \vdots & \vdots & \vdots & \ddots
\end{array}\right]. \tag{27}$$

For a zero coupling J, the Hamiltonian is diagonal with the time-dependent eigenvalues $E^{(\mathrm{d})}_{m\pm}(t) = m\omega \pm \lambda t$ and the corresponding eigenstates are the diabatic states $|\psi^{(\mathrm{d})}_{m\pm}\rangle$. The analytical expressions for the adiabatic states $|\psi^{(\mathrm{ad})}_{m\pm}(t)\rangle$ are complicated [9], but the expressions for the adiabatic energies are rather simple,

$$E^{(\mathrm{ad})}_{m\pm}(t) = \pm\frac{\omega}{2\pi}\cos^{-1}\left(\frac{\omega^2-\pi^2J^2}{\omega^2+\pi^2J^2}\cos\frac{2\pi\lambda t}{\omega}\right) + m\omega. \tag{28}$$

The diabatic energies forms a grid in the E-t plane with repeated exact crossings at the instants $t_j = j\tau_{\mathrm{per}}/2$ for integers j and the period $\tau_{\mathrm{per}} = \omega/\lambda$. A nonzero J couples every positive diabatic state to every negative diabatic state with equal strengths. This implies that every crossing becomes avoided with a gap $\sim 2J$. These form the adiabatic energies which are shown in Fig. 3 together with the diabatic energies. It is convenient to relabel the adiabatic states with a collective index l such that $m+ \leftrightarrow 2l$ and $m- \leftrightarrow 2l+1$.

There are a few interesting observations to be made regarding the adiabatic energies Eq. (28): (i) for $J = \omega/\pi$ the energies become $E^{(\mathrm{ad})}_l(t) = \frac{\omega}{2}(l+\frac{1}{2})$ (using the relabeling of the adiabatic states/energies), i.e., time-independent and forming a (Wannier-Stark–like) ladder, and (ii) a grid structure emerges also for strong coupling $|J| > \omega/\pi$ that is very

similar to that of the figure apart from that it is shifted by half a period. A consequence of the second property is that the evolution becomes highly nonadiabatic also for $J \gg \omega$.

Another important property of the model is its periodicity, which is somewhat hidden. It is clear that the adiabatic spectrum is periodic with the period τ_{per}, but the diabatic energies have a linear time-dependence and does not seem periodic. The periodicity in the diabatic representation translates into $E^{(\text{d})}_{(m\mp1)\pm}(t) = E^{(\text{d})}_{m\pm}(t + \tau_{\text{per}})$. Thus, if time is shifted by τ_{per} simultaneously as the energy index is shifted by -1 the spectrum is invariant. This is a true identity since the spectrum is assumed unbounded both from below and above.

If we assume that the avoided crossings are well separated it is justified to consider nonadiabatic transitions only between neighboring adiabatic states. We may then approximate a single crossing by a two-level Landau-Zener model [22]. Given that the system resides in a single diabatic state before the crossing the Landau-Zener formula $P_{\text{D}} = \exp(\pi J^2/\lambda)$ gives the probability for population transfer to the other diabatic state. The full time-evolution of the system can be seen as a grid of repeated Landau-Zener crossings. If initially, say, the system is prepared in a single diabatic or adiabatic state, as the system goes through repeated crossings, one would expect continued broadening of the energy uncertainty $\Delta E(t) = \sqrt{\langle\psi(t)|(\hat{H}^{(\text{d})}_{\text{LZg}}(t))^2|\psi(t)\rangle - \langle\psi(t)|\hat{H}^{(\text{d})}_{\text{LZg}}(t)|\psi(t)\rangle^2}$. However, interferences between the different "paths" that the system takes through the grid should somehow influence the overall dynamics. In fact, the system is a sort of multistate Landau-Zener-Stückelberg interferometer [24]. Thus, the evolution is reminiscent of a discrete quantum walk [25]: the nonadiabatic transitions play the role of moving the walker to the right/left (for us up/down in energy). For a discrete quantum walk the spreading is super-diffusive (ballistic), $\Delta E \sim t$, in contrast to a classical walker that is diffusive, $\Delta E \sim \sqrt{t}$. The difference with a standard discrete quantum walk is that the different paths result in different dynamical phases, which we know is the reason for the Bloch revival. So the constructive interference that causes the state to relocalize will counteract the spreading of the wave-packet. Indeed, for short times we do find a super-diffusive spreading like in a quantum walk, and also the probability distribution Eq. (17) resembles that of a discrete quantum walk [25]. But over longer times we see instead the Bloch oscillations.

On average the distance between the adiabatic energies is $\omega/2$ which should reproduce a Bloch period of $T_{\text{EBloch}} = 4\pi/\omega$. To see the Bloch oscillations clearly, we require that this period is larger than the period $\tau_{\text{per}} = \omega/\lambda$ of our model; see Fig. 3. As discussed in the previous section, when this is true we may time-average $E^{(\text{ad})}_n(t)$ and $\Theta_1(t)$ to get an exact mapping between our model and the single-band Bloch Hamiltonian Eq. (1). Figure 4(a) displays the results for a numerical simulation of our model in this parameter regime. We indeed see energy Bloch oscillations with the correct period, even though the revival is not perfect. Furthermore, the shape of this breathing mode is not exactly like that of Fig. 1(a). This can be ascribed to the explicit time-dependence of the system parameters together with coupling terms beyond nearest neighboring adiabatic states.

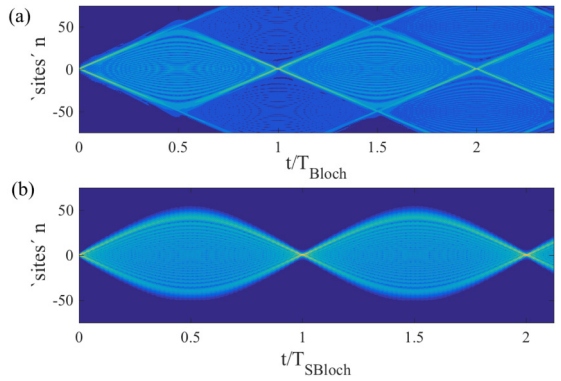

FIG. 4. Demonstration of the energy Bloch oscillations (a) and super energy Bloch oscillations (b) in the Landau-Zener grid model. In both cases we show the breathing mode, the oscillating mode does not show as clear oscillating structures. As for Fig. 2, the plots show $\sqrt{P_n(t)}$, see Eq. (17), for the different adiabatic states, and with the initial state only populating the middlemost adiabatic state. The periodic evolution is evident even though there are differences compared to Fig. 1. Especially interesting is that for the energy Bloch oscillations, the structure of the breathing model is more diamond-shaped than for regular Bloch oscillation [see Fig. 1 (a)]. In (a) it is evident that some population is "leaking out" causing incomplete revivals (even though it should be remembered that we plot $\sqrt{P_n(t)}$ for visibility and not $P_n(t)$ such that the weakly populated states get "magnified"). The energy Bloch period is simply $T_{\text{EBloch}} = 4\pi/\omega$ (4π since the level spacing is $\omega/2$ and not ω), while the super energy Bloch oscillation period is found numerically to $T_{\text{sEBloch}} \approx 2300/\omega$. In both plots $\lambda = 1$, while the other dimension parameters are $\omega = 0.5$ and $J = 0.2$ in (a), and $\omega = 5$ and $J = 0.5$ in (b).

The fact that the parameters have a periodic time-dependence suggests that our model is like a driven tilted lattice, and hence, it should also be possible to see super Bloch oscillations. Those should occur with a period typically much larger than T_{EBloch} and τ_{per}. By increasing ω we are no longer in the Bloch oscillating regime $T_{\text{EBloch}} \ll \tau_{\text{per}}$, and we then find breathing modes with much larger periods; see Fig. 4(b). To compare the different timescales in our system is harder than for a driven tight-binding Bloch model, and as a consequence it is not as easy to identify the period. Nevertheless, we find a beating between T_{sEBloch} and τ_{per} – perfect revivals only occurs when the $T_{\text{sEBloch}}/\tau_{\text{per}}$ is an integer. In addition, we have verified numerically that $T_{\text{sEBloch}} \sim 1/\omega$ (the proportionality constant for the example of Fig. 4(b) is roughly 2300, which can be compared to 4π for the regular Bloch oscillations).

IV. PREPARATION OF CAT STATES

Returning to the Sec. II A of the single-band tight-binding model. According to the acceleration theorem, the motion of the wave-packet, when localized in momentum, is determined by the group velocity. We note that if the tunneling amplitude J swaps sign, so will the group velocity since the band $\varepsilon(k)$ is flipped up-side-down. This fact is used in the following where we propose how to prepare motional cat states in a trapped ion system [16].

An advantage with the trapped ion setup is the flexibility in monitoring desirable Hamiltonians by driving different motional sidebands [16]. In particular, a two-level ion in a harmonic trap is illuminated with a coherent laser. The laser drives the transition between the two internal states $|\pm\rangle$. Simultaneously, the momentum carried by absorbed and emitted photons may induce creation or annihilation of ionic vibration excitations. To avoid internal transitions between the states $|\pm\rangle$, the laser is assumed to be far detuned from these transitions. Due to the internal ionic transitions being far detuned from the applied laser, it is implied that we consider the generalized driven harmonic oscillator Hamiltonian

$$\hat{H}_{\rm Ion}(t) = \omega\hat{a}^\dagger\hat{a} + J\frac{\hat{a}^\dagger + \hat{a}}{\sqrt{2}}\sin(\Omega t)\hat{\sigma}_z, \tag{29}$$

where $\hat{\sigma}_z|\pm\rangle = \pm|\pm\rangle$. Thus, whether the ion is in the lower $|-\rangle$ or upper $|+\rangle$ internal state will determine the sign of the driving term. From Eq. (24) we have that such a sign change will also flip the sign of the tunneling amplitude in the corresponding lattice model. Accordingly, we expect opposite group velocities depending on the internal $|\pm\rangle$ states.

Before demonstrating the outcome of having opposite signs of J, we briefly mention what we mean by a "cat state" [26]. The superposition of "dead" and "alive" implies that the corresponding states, $|\psi_+\rangle$ and $|\psi_-\rangle$, should not only be orthogonal but also well separated in a phase space sense. In the seminal work on preparing cat states in cavity QED [27], the cat comprises a superposition of two photonic coherent states with equal amplitude but different phases. The resulting cat state has the form $|\psi\rangle = \frac{1}{\sqrt{N}}(|\alpha e^{i\phi}\rangle|+\rangle + |\alpha e^{-i\phi}\rangle|-\rangle)$, where N is a normalization constant, α is the coherent state amplitude, ϕ the coherent state phase, and $|\pm\rangle$ the two internal atomic states which are used to prepare the cat. To call this state a cat one should have $|\alpha|^2 \gg 1$ and $\langle\alpha e^{i\phi}|\alpha e^{-i\phi}\rangle \approx 0$. We note that the atom is then approximately maximally entangled with the photon field.

Returning to our system, we consider the initial state

$$|\psi\rangle = |\varphi\rangle\frac{1}{\sqrt{2}}(|+\rangle + |-\rangle), \tag{30}$$

where $|\varphi\rangle$ is some initial motional state, and propagate it for a time $t = T_{\rm sEBloch}/2$ with the Hamiltonian Eq. (29), leading to a state $|\psi(T_{\rm sEBloch}/2)\rangle = \frac{1}{\sqrt{N}}(|\varphi_+\rangle|+\rangle + |\varphi_-.\rangle|-\rangle)$. The result for a coherent state $|\varphi\rangle = |\beta\rangle$ is presented in Fig. 5(a) by showing the Husimi Q-function defined as

$$Q(\alpha) = \frac{1}{\pi}\langle\alpha|\hat{\rho}_{\rm phon}|\alpha\rangle, \tag{31}$$

with $\hat{\rho}_{\rm phon} = \frac{1}{N}(|\varphi_+\rangle\langle\varphi_+| + |\varphi_-\rangle\langle\varphi_-|)$ the reduced density operator for the ion's motional state and $|\alpha\rangle$ a coherent state with complex amplitude $\alpha = x + ip$. The splitting between the two states $|\varphi_\pm\rangle\langle\varphi_\pm|$ is evident, as is the fact that the two states have different amplitudes (i.e., the average number of phonons differ for the two states, which follows since one of the states climbs up the energy ladder while the other climbs down). Note further that the two-phase space blobs are Gaussian. In fact, the resulting cat is composed of two coherent states since under time-evolution of the corresponding driven harmonic oscillator an initial coherent remains coherent [7].

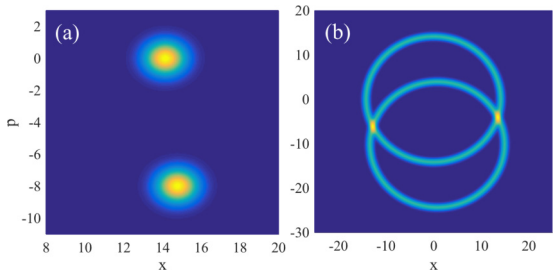

FIG. 5. The motional Q-function Eq. (31) at half the super Bloch period $T_{\rm sEBloch}/2$ for the initial state Eq. (30) with either a coherent state, $|\varphi\rangle = |\beta\rangle$ (a), or a Fock state, $|\varphi\rangle = |n\rangle$ (b). By considering an initial coherent state we regain Bloch oscillating evolution as in Fig. 2(b), while an initial Fock state generates the breathing motion evolution as in Fig. 2(a). Interestingly, the characteristic phase space features of the two states, Gaussian for a coherent state and ring-shaped for a Fock state, survive the evolution. In both cases the two states are well separated with approximately zero overlap $\langle\varphi_+|\varphi_-\rangle \approx 0$. The parameters are as in Figs. 2(a) and 2(b) except $\Omega = 1.05$, which results in a larger Bloch oscillating amplitude and thereby larger phase space separation between the two states.

The other scenario when we initialize the ion in a Fock state is also interesting in terms of state preparation. In the standard Bloch oscillation setup this corresponds to populating all quasimomentum states of the band. The group velocity argument above does not make sense in this situation. Nevertheless, the motional states still split up in two parts in phase space, as depicted in Fig. 5(b). It suggests that the two states $|\varphi_\pm\rangle\langle\varphi_\pm|$ are now displaced Fock states [21], i.e., the characteristic ring shape of the Q-function for a Fock state persists but has been displaced from the origin. However, a closer analysis shows that this observation is not exact, even though many of the properties of displaced Fock states are also carried by the states $|\varphi_\pm\rangle\langle\varphi_\pm|$. By changing the parameters in the simulation it is possible to make the two "rings" of the Q-function in Fig. 5(b) to not overlap at all. Whether this state should be called a cat state is questionable; on the one hand, the two parts can be well separated in phase space, but on the other hand, the two constituting parts are nonclassical in nature (contrary to large amplitude coherent states).

V. CONCLUDING REMARKS AND DISCUSSIONS

By considering a class of periodically driven quantum systems we have shown how perfect oscillating dynamics can emerge. There is a mapping from these systems to the tilted single-band model, which identifies the periodic behavior as Bloch oscillations. This type of Bloch oscillations appear in the space of adiabatic states. Hence, the system's instantaneous energy oscillates in time. This phenomenon was verified by exploring two different models. The first is a trivial driven harmonic oscillator, and the periodic evolution is perfect in this case. In a strict sense, the obtained Bloch oscillations are super Bloch oscillations which appear in driven tilted Bloch oscillating systems as a beating mechanism between different frequencies. The second model, a Landau-Zener grid, consists in repeated Landau-Zener crossings which forms a grid in the energy-time plane. When given

in the diabatic basis this model is not manifestly periodic in time, but rather describe a linear quench. However, this is only true in this particular basis. In the adiabatic basis, for example, the periodicity becomes clear. For this model, the energy Bloch oscillations are not as perfect, but they still dominate the evolution. When the "translational invariance", imposed by the instantaneous equidistant spectrum, is broken by a random "disorder" we saw a breakdown of the energy Bloch oscillations and a buildup of diffusive spreading.

Using trapped ion physics we proposed how to employ the energy Bloch oscillations to prepare Schrödinger cat states, i.e., superpositions of states well separated in phase space. In particular, with an initial coherent vibrational state of the ion, after half a Bloch period the ion's motional state is in a superposition of two coherent states. Similar ideas should be applicable also in cavity (circuit) QED setups.

The energy Bloch oscillations should be fairly straightforward to verify experimentally in various realizations of driven harmonic oscillators. We already in the text suggested trapped ion systems for this purpose [16]. The trapping potential is to a good approximation harmonic up to hundreds of phonons and the periodic driving is rather straightforward by tuning the laser frequency to the correct sidebands. Naturally, the Bloch period T_{EBloch} should be considerably smaller than the characteristic timescales for possible dissipation of decoherence regardless of system considered. As a coherent interference phenomenon, any decoherence will demolish the oscillations. For trapped ions the characteristic frequency is on the MHz scale, while motional heating rate and ionic spontaneous emission rate of the excited state $|+\rangle$ are both on the Hz scale such that they can be completely ignored [28]. Some decoherence arises also from fluctuations in the trap parameters, but these are assumed small on the interesting timescales. Another property of trapped ions is that it is possible to initialize highly excited Fock states [29] needed if one studies the breathing modes. For a driven high-Q cavity photon losses are inevitably present, but by considering realistic experimental parameters one finds that this should not cause any problems. The lifetime for a microwave cavity photon can be as large as tenth of ms, and the photon frequency $\omega \sim 50$ GHz [30]. Thus, it should be enough to drive the cavity with a detuning $\delta\Omega = \Omega - \omega$ around MHz. In the cavity setup is should be especially easy to detect the energy Bloch oscillations by simply detecting the characteristics of the cavity output field. Already the field intensity $\langle \hat{n}_{\mathrm{out}} \rangle$ will be oscillating with the Bloch period.

To experimentally realize the Landau-Zener grid model would require a bit more work. As expressed in Eq. (26) we have a large spin coupled to a qubit. We can alternatively replace the large spin with a harmonic oscillator, and the model is sort of a generalized quantum Rabi model [31] with a very special "light-matter" coupling. The system with maybe the largest freedom in engineering such a coupling is that of trapped ions [16]. The desired coupling according to the Hamiltonian Eq. (26) should include every possible phonon transition; single phonon, two phonons, and so on. This is certainly challenging, but we do not rule it out.

ACKNOWLEDGMENTS

We thank Markus Hennrich and José Suarez Huayra for helpful discussions. We acknowledge financial support from the Knut and Alice Wallenberg foundation (KAW) and the Swedish research council (VR).

[1] P. Ponte, A. Chandrana, Z. Papic, and D. A. Abanin, Ann. Phys. **353**, 196 (2015); V. Khemani, A. Lazarides, R. Moessner, and S. L. Sondhi, Phys. Rev. Lett. **116**, 250401 (2016).

[2] M. O. Scully and M. S. Zubairy, *Quantum Optics* (Cambridge University Press, Cambridge, 1997).

[3] M. Glück, A. R. Kolovsky, and H. J. Korsch, Phys. Rep. **366**, 103 (2002).

[4] C. Waschke, H. G. Roskos, R. Schwedler, K. Leo, H. Kurz, and K. Köhler, Phys. Rev. Lett. **70**, 3319 (1993); M. Ben Dahan, E. Peik, J. Reichel, Y. Castin, and C. Salomon, *ibid.* **76**, 4508 (1996); R. Morandotti, U. Peschel, J. S. Aitchison, H. S. Eisenberg, and Y. Silberberg, *ibid.* **83**, 4756 (1999); G. Ferrari, N. Poli, F. Sorrentino, and G. M. Tino, *ibid.* **97**, 060402 (2006); H. Keßler, J. Klinder, B. P. Venkatesh, C. Georges, and A. Hemmerich, New J. Phys. **18**, 111005 (2016).

[5] K. Kudo and T. S. Monteiro, Phys. Rev. A **83**, 053627 (2011).

[6] E. Haller, R. Hart, M. J. Mark, J. G. Danzl, L. Reichsollner, and H.-C. Nägerl, Phys. Rev. Lett. **104**, 200403 (2010).

[7] K. Husimi, Prog. Theor. Phys. **9**, 381 (1953).

[8] Y. N. Demkov and V. N. Ostrovsky, J. Phys. B **28**, 403 (1995).

[9] Y. N. Demkov, P. B. Kurasov, and V. N. Ostrovsky, J. Phys. A **28**, 4361 (1995).

[10] D. A. Harmin, Phys. Rev. A **56**, 232 (1997).

[11] V. Grecchi and A. Sacchetti, Phys. Rev. B **63**, 212303 (2001).

[12] T. Hartmann, F. H. Keck, J. Korsch, and S. Mossmann, New J. Phys. **6**, 2 (2004).

[13] M. Holthaus and D. W. Hone, Philos. Mag. B **74**, 105 (1996).

[14] A. Eckardt, M. Holthaus, H. Lignier, A. Zenesini, D. Ciampini, O. Morsch, and E. Arimondo, Phys. Rev. A **79**, 013611 (2009).

[15] K. W. Madison, M. C. Fischer, R. B. Diener, Q. Niu, and M. G. Raizen, Phys. Rev. Lett. **81**, 5093 (1998); A. R. Kolovsky and H. J. Korsch, arXiv:0912.2587.

[16] D. Leibfried, R. Blatt, C. Monroe, and D. Wineland, Rev. Mod. Phys. **75**, 281 (2003).

[17] A. Bohm, A. Mostafazadeh, H. Koizumi, Q. Niu, and J. Zwanziger, *The Geometric Phase in Quantum Systems: Foundations, Mathematical Concepts, and Applications in Molecular and Condensed Matter Physics* (Springer, Berlin, 1993).

[18] M. Baer, *Beyond Born-Oppenheimer: Electronic Nonadiabatic Coupling Terms and Conical Intersections* (John Wiley & Sons, New York, 2006).

[19] M. Grifoni and P. Hänggi, Phys. Rep. **304**, 229 (1998).

[20] L. Allen and J. H. Eberly, *Optical Resonance and Two-level Atoms* (Dover Publications, Mineola, NY, 1987).

[21] F. A. M. de Oliveira, M. S. Kim, P. L. Knight, and V. Buek, Phys. Rev. A **41**, 2645 (1990).
[22] L. Landau, Phys. Zeitschrift Sowjetunion **2**, 46 (1932); C. Zener, Proc. R. Soc. London A **137**, 696 (1932).
[23] C. E. Carroll and F. T. Hioe, J. Phys. A **19**, 2061 (1986); V. N. Ostrovsky and H. Nakamura, *ibid.* **30**, 6939 (1997); M. V. Volkov and V. N. Ostrovsky, J. Phys. B **37**, 4069 (2004); J. Larson, Europhys. Lett. **107**, 30007 (2014).
[24] S. N. Shevchenko, S. Ashhab, and F. Nori, Phys. Rep. **492**, 1 (2010).
[25] J. Kempe, Contemp. Phys. **44**, 307 (2003).
[26] J.-M. Raimond and S. Haroche, *Exploring the Quantum* (Oxford University Press, Oxford, 2006).
[27] M. Brune, E. Hagley, J. Dreyer, X. Maître, A. Maali, C. Wunderlich, J. M. Raimond, and S. Haroche, Phys. Rev. Lett. **77**, 4887 (1996).
[28] C. Hempel, B. P. Lanyon, P. Jurcevic, R. Gerritsma, R. Blatt, and C. F. Roos, Nat. Photon. **7**, 630 (2013).
[29] C. Schäfermeier *et al.*, Nat. Commun. **7**, 13628 (2016); Fabian Wolf, C. Shi, J. C. Heip, M. Gessner, L. Pezzè, A. Smerzi, M. Schulte, K. Hammerer, and P. O. Schmidt, arXiv:1807.01875.
[30] S. Deléglise, I. Dotsenko, C. Sayrin, J. Bernu, M. Brune, J.-M. Raimond, and S. Haroche, Nature **455**, 510 (2008).
[31] J. Larson, Phys. Scr. **76**, 146 (2007); references in D. Braak, Q.-H. Chen, M. T. Batchelor, and E. Solano, J. Phys. A **49**, 300301 (2016).